J|A|C|S
ARTICLES
Published on Web 05/23/2002

Measuring Polymer Surface Ordering Differences in Air and Water by Sum Frequency Generation Vibrational Spectroscopy

Jie Wang,[†] Zoltan Paszti,[†,‡] Mark A. Even,[†] and Zhan Chen*[,†]

Contribution from the Department of Chemistry, University of Michigan, 930 North University Avenue, Ann Arbor, Michigan 48109, and Department of Surface Chemistry and Catalysis, Institute of Isotope and Surface Chemistry, MTA Chemical Research Center, P.O. Box 77, H-1525 Budapest, Hungary

Received October 18, 2001

Abstract: Molecular structures of poly(*n*-butyl methacrylate) (PBMA) at the PBMA/air and PBMA/water interfaces have been studied by sum frequency generation (SFG) vibrational spectroscopy. PBMA surfaces in both air and water are dominated by the methyl groups of the ester side chains. The average orientation and orientation distribution of these methyl groups at the PBMA/air and PBMA/water interfaces are different, indicating that surface restructuring occurs when the PBMA sample contacts water. Analysis shows that the orientation distribution of side chain methyl groups on the PBMA surface is narrower in water than that in air, indicating that the PBMA surface can be more ordered in water. To our knowledge, this is the first time that quantitative comparisons between molecular surface structures of polymers in air and in water have been made. Two assumptions on the orientation distribution function, including a Gaussian distribution and a formula based on the maximum entropy approach, are used in the analysis. It has been found that the orientation angle distribution function deduced by the Gaussian distribution and the maximum entropy distribution are quite similar, showing that the Gaussian distribution is a good approximation for the angle distribution. The effect of experimental error on the deduced orientational distribution is also discussed.

1. Introduction

The performance of many polymers is often dictated by their surface or interface properties, such as wettability, friction, lubricity, wearability, adhesion, and biocompatibility.[1−4] Such properties depend critically upon the molecular structure at the polymer surface or interface; thus, it is crucial to understand polymer surface or interface structures at the molecular level. In recent years, sum frequency generation (SFG) vibrational spectroscopy has been successfully developed into a powerful and unique technique to study molecular structures of surfaces and interfaces.[5−15] It has been applied to study polymer surface structures in air,[16−18] modification of polymer surfaces by surface treatment,[19,20] surface structures of polymer blends,[21] and restructuring of polymer surfaces in aqueous solution.[22,23]

One of the advantages of using SFG to study surface structures is that orientation and orientation distribution of surface functional groups can be possibly deduced by collecting SFG spectra using different polarization combinations of input and output beams;[24−27] thus, information of surface structure can be obtained. Another advantage of SFG is that it can detect

* To whom all correspondence should be addressed. E-mail: zhanc@umich.edu. Fax: 734-647-4865.

[†] University of Michigan.

[‡] Institute of Isotope and Surface Chemistry, MTA Chemical Research Center.

(1) Andrade, J. D. *Polymer surface dynamics*; Plenum Press: New York, 1988.
(2) Park, J. B.; Lakes, R. S. *Biomaterials: An Introduction*; Plenum Press: New York, 1992.
(3) Carbassi, F.; Morra, M.; Occhiello, E. *Polymer Surfaces: From Physics to Technology*; John Wiley and Sons: Chichester, 1994.
(4) Feast, W. J.; Munro, H. S.; Richards, R. W. *Polymer Surfaces and Interfaces II*; John Wiley and Sons: New York, 1992.
(5) Shen, Y. R. *The Principles of Nonlinear Optics*; Wiley: New York, 1984.
(6) Shen, Y. R. *Annu. Rev. Phys. Chem.* **1989**, *40*, 327.
(7) Guyot-Sionnest, P.; Hunt, J. H.; Shen, Y. R. *Phys. Rev. Lett.* **1987**, *59*, 1597.
(8) Bain, C. D. *J. Chem. Soc., Faraday Trans.* **1995**, *91*, 1281.
(9) Eisenthal, K. B. *Chem. Rev.* **1996**, *96*, 1343.
(10) Walker, R. A.; Gruetzmacher, J. A.; Richmond, G. L. *J. Am. Chem. Soc.* **1998**, *120*, 6991.
(11) Scatena, L. F.; Brown, M. G.; Richmond, G. L. *Science* **2001**, *292*, 908.
(12) Chen, Z.; Gracias, D. H.; Somorjai, G. A. *Appl. Phys. B* **1999**, *68*, 549.
(13) Shultz, M. J.; Schnitzer, C.; Simonelli, D.; Baldelli, S. *Int. Rev. Phys. Chem.* **2000**, *19*, 123.
(14) Kim, J.; Cremer, P. S. *J. Am. Chem. Soc.* **2000**, *122*, 12371.
(15) Pizzolatto, R. L.; Yang, Y. J.; Wolf, L. K.; Messmer, M. C. *Anal. Chim. Acta* **1999**, *397*, 81.
(16) Briggman, K. A.; Stephenson, J. C.; Wallace, W. E.; Richter, L. J. *J. Phys. Chem B* **2001**, *105*, 2785.
(17) Gautam, K. S.; Schwab, A. D.; Dhinojwala, A.; Zhang, D.; Dougal, S. M.; Yeganeh, M. S. *Phys. Rev. Lett.* **2000**, *85*, 3854.
(18) Chen, Z.; Ward, R.; Tian, Y.; Baldelli, S.; Opdahl, A.; Shen, Y. R.; Somorjai, G. A. J. Am. Chem. Soc. **2000**, *122*, 10615.
(19) Zhang, D.; Dougal, S. M.; Yeganeh, M. S. *Langmuir* **2000**, *16*, 4528.
(20) Kim, D.; Shen, Y. R. *Appl. Phys. Lett.* **1999**, *74*, 3314.
(21) Chen, Z.; Ward, R.; Tian, Y.; Eppler, A. A.; Shen, Y. R.; Somorjai, G. A. *J. Phys. Chem. B.* **1999**, *103*, 2935.
(22) Zhang, D.; Ward, R. S.; Shen, Y. R.; Somorjai, G. A. *J. Phys. Chem.* **1997**, *101*, 9060.
(23) Wang, J.; Woodcock, S. E.; Buck, S. M.; Chen, C. Y.; Chen, Z. *J. Am. Chem. Soc.* **2001**, *123*, 9470; details of the experimental geometry and discussions about selective probe of polymer/air and polymer/water interfaces are shown in the Supporting Information.
(24) Hirose, C.; Akamatsu, N.; Domen, K. *J. Chem. Phys.* **1992**, *96*, 997.
(25) Hirose, C.; Yamamto, H.; Akamatsu, N.; Domen, K. *J. Phys. Chem.* **1993**, *97*, 10064.
(26) Hirose, C.; Akamatsu, N.; Domen, K. *Appl. Spectrosc.* **1992**, *46*, 1051.
(27) Zhuang, X.; Miranda, P. B.; Kim, D.; Shen, Y. R. *Phys. Rev. B.* **1999,** *59*, 12632.

10.1021/ja012387r CCC: $22.00

molecular interface structures directly from the "buried" solid/liquid interface. Therefore, surface structures can be compared in air and in water by SFG studies.

On an ordered surface, the orientation of surface functional groups can be assumed to be a δ angle distribution; therefore, the orientation angle(s) can be deduced by using the intensity ratio of SFG spectra collected with different polarization combinations of input and output laser beams. If the assumption of a very narrow angle distribution cannot be confirmed by separate measurements, evaluation of the orientation distribution is equally important. If, for example, the orientation angle is deduced to be close to the so-called "magic angle", it is difficult to identify whether it is the real orientation angle, since various angles with different angle distributions would give the same result.[28]

Polymer surfaces are usually considered to be less ordered. Understanding and controlling orientation distribution of surface functional groups or surface structural ordering of polymer materials is very important. For example, a polymer surface with well-aligned polymer chains could serve as a template for growing highly ordered polymeric or organic crystals with superb mechanical, electrical, thermal, or optical properties.[29] We believe that information about polymer surface ordering will provide a new view and a new understanding of polymer surface structures for scientists in many different areas. Information on orientation distribution can be obtained either from additional SFG measurements or other sources. Shen and his colleagues have studied orientation and orientation distribution of methylene groups on a rubbed poly(vinyl alcohol) (PVA) surface using absolute SFG intensities and found that it was quite ordered due to mechanical rubbing.[30] On the other hand, Simpson et al. have compared data obtained from second harmonic generation and linear optical methods to determine the angular distribution of surface-bound molecular systems.[31] For the polymer system presented here, linear optical investigation methods are not applicable because of the lack of surface sensitivity.

Previously we have demonstrated at the molecular level by SFG that surface restructurings of poly(methacrylate)s with various side chains in water are quite different. Qualitative results of these surface restructurings in water have been summarized in a recent communication.[23] Here we present an in-depth investigation of the surface restructuring of PBMA in water. The orientation and orientation distribution of side chain methyl groups on PBMA surface in air and water have been quantified by using both the spectral intensity ratio of SFG spectra collected with different polarization combinations of input and output laser beams, and the absolute SFG spectral intensity which has been calibrated by a known standard z-cut quartz. We determined the structural ordering of the PBMA surface in air and in water by comparing the orientation angle distributions of side chain methyl groups. The surface orientation angle distribution was calculated by using both a Gaussian distribution and a more general distribution obtained from the maximum entropy approach (we will refer to it as "maximum entropy distribution" below). According to the results, we have demonstrated by SFG for the first time that a polymer surface structure can be more ordered in water than that in air.

(28) Simpson, G. J.; Rowlen, L. K. *J. Am. Chem. Soc.* **1999**, *121*, 2635.
(29) Wittmann, J. C.; Smith, P. *Nature* **1991**, *352*, 414.
(30) Wei, X.; Zhuang, X.; Hong, S. C.; Goto, T.; Shen, Y. R. *Phys. Rev. Lett.* **1999**, *82*, 4256.
(31) Simpson, G. J.; Westerbuhr, S. G.; Rowlen, K. L. *Anal. Chem.* **2000**, *72*, 887.

2. Experimental Setup

Polymer samples investigated in this work were prepared using PBMA (MW = 180 000, purchased from Scientific Polymer Products Inc., used as received). Films were obtained by spin coating 2 wt % polymer/toluene solution at 3000 rpm on fused silica substrates (1 in. diameter, 1/8 in. thick, purchased from ESCO products). Samples were annealed at 80 °C for 20 h before analysis. The film thickness was measured to be about 100 nm by a Dektak 3 profilometer.

The SFG spectra shown in this paper were collected by a custom designed EKSPLA SFG spectrometer, which was described in detail elsewhere.[23,32] Briefly, the visible input beam at 0.532 μm was generated by doubling a part of the fundamental output from an EKSPLA Nd:YAG laser. The IR beam tunable between 2.5 and 10 μm (with a line width $< 6\ cm^{-1}$) is obtained from an optical parametric generation/amplification/difference frequency generation (OPG/OPA/DFG) system based on LBO and $AgGaS_2$ crystals, which were pumped by the third harmonic and the fundamental output of the laser. Both beams had a pulse width of ~20 ps, a repetition rate of 20 Hz, and a typical beam diameter of ~0.5 mm at the sample surface. The incident angles of the visible beam and the IR beam were 60° and 54°, and their energies at the sample surface were ~300 and ~100 μJ, respectively.

For the present investigations two sample geometries were used. In the "sample face up" arrangement (polymer film on top) we collected SFG spectra of the air/polymer interface in the reflection direction from the top of the sample. In the "sample face down" geometry (fused silica substrate on top), the input beams traveled through the substrate and were overlapped at the polymer/air interface. We collected the reflected SFG spectra generated from that interface through the substrate.[23] The SFG spectra tested with both geometries were identical except that the spectral intensities were different, due to the different Fresnel coefficients and other parameters in eq 3.1 (see below). This latter arrangement can bring the polymer film in contact with water and collect SFG spectra from the polymer/water interface.[23]

3. Theoretical Background

The SFG output in terms of energy per pulse in the reflected direction can be written as[27]

$$S(\omega) = \frac{8\pi^3\omega^2 \sec^2\beta}{c^3 n_1(\omega) n_1(\omega_1) n_1(\omega_2)} |\chi^{(2)}_{\text{eff}}|^2 I_1(\omega_1) I_2(\omega_2) AT \quad (3.1)$$

where $n_1(\omega_i)$ is the refractive index of the incident medium at frequency ω_i, ω and β are the frequency and the reflection angle of the sum frequency field, respectively, $I_1(\omega_1)$ and $I_2(\omega_2)$ are the intensities of the two input fields with frequencies ω_1 and ω_2, T is the pulse-width of both input lasers, A is the overlapping cross section of the two input beams at the sample, and $\chi^{(2)}_{\text{eff}}$ is the effective second-order nonlinear susceptibility.

The effective second-order nonlinear susceptibility tensor of the surface, $\chi^{(2)}_{\text{eff}}$, is related to the second-order nonlinear susceptibility tensor $\chi^{(2)}$ in the lab coordinate system. In this report, we have collected SFG spectra with two polarization combinations of input and output laser beams, namely, ssp (s-polarized SFG output, s-polarized visible input, p-polarized infrared input) and sps. The two measured components of $\chi^{(2)}_{\text{eff}}$ are related to the tensor components $\chi^{(2)}_{ijk}$ ($i, j, k = x, y, z$) of $\chi^{(2)}$ (see, for example, ref 27) by:

$$\chi^{(2)}_{\text{eff,ssp}} = F_{\text{ssp}}\chi^{(2)}_{yyz}$$
$$\chi^{(2)}_{\text{eff,sps}} = F_{\text{sps}}\chi^{(2)}_{yzy} \quad (3.2)$$

where F_{ssp} and F_{sps} are the Fresnel coefficients, $\chi^{(2)}_{yyz}$ and $\chi^{(2)}_{yzy}$ are different components of $\chi^{(2)}$ with the lab coordinates chosen in such a way that z is along the interface normal and x is in the plane of incidence. $\chi^{(2)}_{yyz}$ and $\chi^{(2)}_{yzy}$ can be written as:

$$\chi^{(2)}_{ijk} = \chi^{(2)}_{NR} + \sum_q \chi^{(2)}_{ijk,q} = \chi^{(2)}_{NR} + \sum_q \frac{A_{ijk,q}}{\omega_2 - \omega_q + i\Gamma_q} \qquad (3.3)$$

where χ_{NR} arises from the nonresonant background contribution, and A_q, ω_q and Γ_q are the strength, resonant frequency, and damping coefficient of the qth vibrational mode, respectively.

To deduce orientation information of methyl groups on the PBMA surface from the measured ssp and sps SFG spectra, we made some general assumptions. The methyl group can usually be treated as having C_{3v} symmetry. It is reasonable to assume that the polymer surface is azimuthally isotropic; therefore, the angle θ between the surface normal and the principal axis of the methyl group can be used to describe its orientation. As mentioned, the polymer surface may not be fully ordered; thus, the molecular orientation can be characterized by the distribution function $f(\theta)$ of the orientation angles.

The measured surface second-order susceptibility tensor elements $\chi^{(2)}_{ijk}$ determined in the laboratory frame (x, y, z) can be expressed in terms of the molecular hyperpolarizability tensor elements α_{abc} described with respect to the molecular frame (a, b, c). The resulting expressions carry the orientation information obtainable from SFG measurements. For the symmetric stretching mode of the methyl group, we have:[26,27]

$$\chi^{(2)}_{yyz,s} = \int_0^\pi \frac{1}{2} N_s \alpha_{ccc,s}[\cos\theta(1+r) - \cos^3\theta(1-r)]\, f(\theta)\sin\theta\, d\theta$$
$$\chi^{(2)}_{yzy,s} = \int_0^\pi \frac{1}{2} N_s \alpha_{ccc,s}[\cos\theta - \cos^3\theta](1-r)\, f(\theta)\sin\theta\, d\theta \qquad (3.4)$$

For the asymmetric stretching mode, we have:

$$\chi^{(2)}_{yyz,as} = \int_0^\pi -\frac{1}{2} N_s \alpha_{caa,as}[\cos\theta - \cos^3\theta]\, f(\theta)\sin\theta\, d\theta$$
$$\chi^{(2)}_{yzy,as} = \int_0^\pi \frac{1}{2} N_s \alpha_{caa,as}\cos^3\theta\, f(\theta)\sin\theta\, d\theta \qquad (3.5)$$

where,

$$\alpha^{(2)}_{abc,q} = \frac{\alpha_{abc,q}}{\omega_2 - \omega_q + i\Gamma_q} \qquad (3.6)$$

and $\alpha_{ccc,s}$, $\alpha_{aac,s}$, $\alpha_{caa,as}$ are nonvanishing stretching vibration hyperpolarizability tensor elements of the methyl group.[24,25] $r = \alpha_{aac,s}/\alpha_{ccc,s}$. N_s is the surface density of methyl groups. From evaluation of eqs 3.4 and 3.5 it follows that the measured tensor elements $\chi^{(2)}_{ijk,q}$ are linear combinations of $\langle\cos\theta\rangle$ (which is $\int_0^\pi \cos\theta\, f(\theta)\sin\theta\, d\theta$) and $\langle\cos^3\theta\rangle$ (which is $\int_0^\pi \cos^3\theta\, f(\theta)\sin\theta\, d\theta$) in the form

$$\chi^{(2)}_{ijk,q} = u_{abc,q}\langle\cos\theta\rangle + w_{abc,q}\langle\cos^3\theta\rangle \qquad (3.7)$$

where coefficients $u_{abc,q}$ and $w_{abc,q}$ are known values related to the molecular hyperpolarizability tensor elements. For simplicity, we can use $\cos\theta$ instead of θ as the independent variable of the distribution. Then the averages can be calculated as

$$\langle\cos^n\theta\rangle = \int_{-1}^{1} \cos^n\theta\, f(\cos\theta)\, d(\cos\theta) \qquad (3.8)$$

which gives the nth moment of the distribution $f(\cos\theta)$.

Therefore, from a mathematical point of view, the problem of determining the molecular orientation is equivalent to reconstructing the distribution function from its first and third moments and the normalization condition. In fact, it is a quite common problem in physics and engineering to determine a function for which only a few moments are known. Examples include calculation of electronic and magnetic structure,[33] determination of thermodynamical functions,[34] and study of tomographic imaging.[35] This task is widely known as the "problem of moments".

It is clear that we can construct an infinite variety of normalized functions for which the first and third moments are equal to the measured values. Therefore, we must make additional assumptions on the form of the distribution function so that we can find a unique and reasonable solution.

Our first assumption is that the distribution function is a Gaussian function:

$$f(\theta) = C\exp\left[-\frac{(\theta-\theta_0)^2}{2\sigma^2}\right] \qquad (3.9)$$

where C is a normalization constant and σ is the root-mean-square width. It follows immediately that if we only measure the intensity ratio of the ssp and sps SFG spectra, we could not get θ_0 and σ at the same time. To deduce θ_0 and σ simultaneously, we also measured the absolute value of $\chi^{(2)}_{yyz,s}$ through measuring the absolute SFG spectral intensity.

Although the Gaussian distribution has been used several times to describe molecular orientation on surfaces[28,30,31] and one can assign a pictorial meaning to its parameters θ_0 and σ, still there is no specific physical reason behind that choice. Indeed, any function that reproduces correctly the first and third moments could be as good a choice as the Gaussian function.

In the treatment of the problem of moments, several methods had been developed for the construction of approximate distribution functions, which—at least in the limit of a huge number of known moments—converge to the real distribution.[33] One of them is the maximum entropy approach, which offers a definite procedure for constructing the distribution. It has its foundation in information theory; that is, it tries to find the least biased form of the distribution, using only the information available from experiment.[36] In this formalism the most probable approximate distribution for each finite N of available moments has the form[36]

$$f(\theta) = \exp\left(\sum_{n=0}^{N} a_n\cos^n\theta\right) \qquad (3.10)$$

This formula is often used in ordering studies of liquid crystals[37] or polymer main chains.[38]

(32) Wang, J.; Chen, C. Y.; Buck, S. M.; Chen, Z. *J. Phys. Chem. B.* **2001**, *105*, 12118.
(33) Mead, L. R.; Papanicolau, N. *J. Math. Phys.* **1984**, *25*, 2404 and references therein.
(34) Poland, D. *J. Chem. Phys.* **2000**, *113*, 9930.
(35) Basu, S.; Bresler, Y. *IEEE Trans. Im. Proc.* **2000**, *9*, 1107.

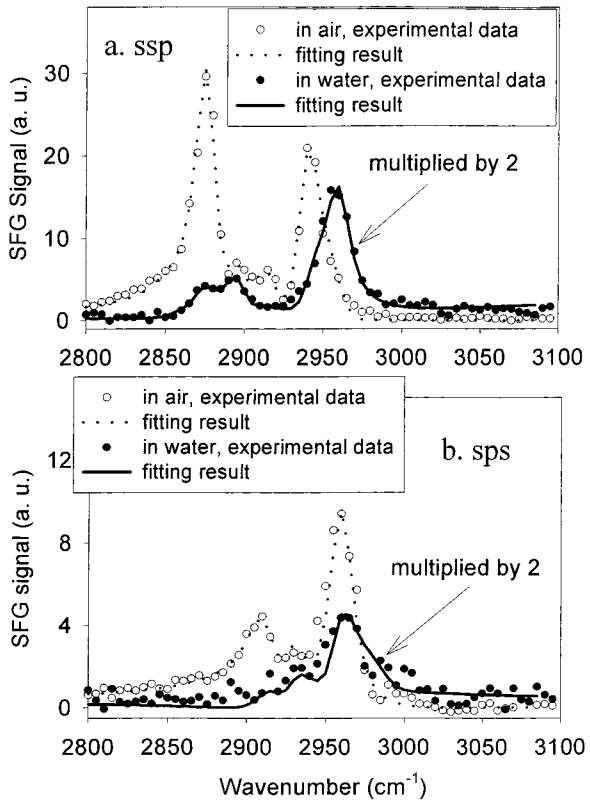

Figure 1. SFG spectra of PBMA in air and water for (a) ssp, (b) sps polarization combinations.

As in the present case we can take into account only two measured quantities, $\langle\cos\theta\rangle$ and $\langle\cos^3\theta\rangle$, and we have to truncate the expression of eq 3.10 at the second-order term:

$$f(\theta) = \exp(a_0 + a_1\cos\theta + a_2\cos^2\theta) \qquad (3.11)$$

To ensure that the Gaussian distribution is a valid approximation for this problem, in the following sections we compare the results of the Gaussian and the maximum entropy approach.

4. Results and Discussion

The ssp and sps SFG spectra of PBMA in air and in water are shown in Figure 1. We have demonstrated by several methods that SFG spectra collected in our experimental geometry come from the polymer/air or polymer/water interface, with almost no contribution from the polymer bulk or polymer/substrate interface.[23] Figure 1 shows that the ssp SFG spectrum in air is dominated by two peaks. The peak at 2875 cm^{-1} is due to the symmetric stretch of the side chain methyl group, and the 2940 cm^{-1} peak is due to Fermi resonance. The 2960 cm^{-1} peak dominates the ssp SFG spectrum of PBMA in water, and the sps spectra of PBMA in both air and water. This peak comes from the asymmetric stretch of the side chain methyl group. There is another peak at 2915 cm^{-1} in the sps spectrum of PBMA in air, with much weaker intensity, due to the asymmetric stretch of the methylene group. The symmetric and asymmetric stretches of the α methyl group are at 2930 and 2990 cm^{-1}, respectively.[32] In the SFG spectra of PBMA in air and water, no strong peaks of the α methyl group on the PBMA surface have been found. It is very clear that the side chain methyl groups dominate all the SFG spectra of PBMA in air and in water. Similar SFG spectra of poly (*n*-butyl acrylate) (also purchased from Scientific Polymer Products Inc., spectrum not shown) compared to those of PBMA also indicate that there is almost no coverage of α methyl groups on the PBMA surface.

Table 1. Measured Second-Order Nonlinear Susceptibility Tensor Components[a]

wavenumber (cm^{-1})	Γ (cm^{-1})	A_{yyz} (A/P)	A_{yyz} (W/P)	A_{yzy} (A/P)	A_{yzy} (W/P)	assignment
2855	6.0	0.44	−1.83	−	−	CH_2(s)
2875	6.0	9.96	7.71	−	−	(ester)CH_3(s)
2895	6.0	3.74	−4.77	−	−	
2915	8.0	5.31	−2.75	3.28	1.79	
2932	8.0	−	4.59	1.77	1.43	
2940	6.0	8.52	7.72	0.36	2.71	Fermi
2960	8.0	−4.78	−12.33	8.06	5.04	(ester)CH_3(as)
2990	10.0	−	−	−	−1.08	(α)CH_3(as)

[a] The unit of A_{ijk} is $\times 10^{-9}$ m^2 V^{-1} s^{-1}. W/P = water/PBMA interface; A/P = air/PBMA interface; s = symmetric stretching vibration; as = asymmetric stretching vibration; Fermi = Fermi resonance.

Comparison of the SFG spectra of PBMA in air and in water shows that when the PBMA surface contacts water, the SFG spectral intensity decreases and the spectral features change dramatically, indicating that the PBMA surface restructures in water. After the sample is removed from water, the spectra recover immediately. After prolonged exposure to water, no additional spectral changes are detected.[23] Therefore, we believe that in water, only the ester chains on the PBMA surface reorganize, and no apparent backbone changes occur. In the following, we discuss the reorientation of side chains on the PBMA surface in water through investigating the orientation distribution of side chain methyl groups on the PBMA surface in air and in water.

As mentioned, the orientation angle and angle distribution cannot be deduced only from the ssp and sps SFG spectral intensity ratio. To deduce the orientation angle and angle distribution of side chain methyl groups on the PBMA surface, we also measured the absolute SFG spectral intensity by comparing the intensity to that of known standard z-cut quartz.[39]

Here we used 1.47 for the refractive index of PBMA and 1.34 for water. The refractive index of the polymer/air interface layer used was 1.24, the average value of the indices of the PBMA and the air. It is very close to the value calculated using formulas from the literature.[27] The refractive index used for the water/polymer interface layer was 1.40, the average value of the indices of the PBMA and the water. We neglected the frequency dependency of any of the refractive indices.

We have fitted the SFG spectra shown in Figure 1 using the method described in section 3. The fitting results after deconvoluting the instrumental resolution are shown in Table 1. Table 1 shows the fitting results with the fewest peaks necessary to obtain a good overlap between the experiment spectrum and the fitted curve. We have tried to fit the spectra by using fewer peaks, but the fitting results did not match the experimental spectra as well as those shown in Figure 1. However, for the best-fitting trials using four peaks in each spectrum, the fitting results of the 2875 and 2960 cm^{-1} (which will be used in the

(36) Tagliani, A. *J. Math. Phys.* **1992**, *34*, 326.
(37) Zannoni, C. in *The Molecular Dynamics of Liquid Crystals*; Luckhurst, G. R., Veracini, C. A., Eds.; NATO Advanced Study Institute Series C431; Kluwer Academic Publishers: Norwell, MA, 1994.
(38) Bower, D. I. *J. Polym. Sci. Polym. Phys. Ed.* **1981**, *19*, 93.
(39) Wei, X.; Hong, S. C.; Zhuang, X. W.; Goto, T.; Shen, Y. R. *Phys. Rev. E* **2000**, *62*, 5160.

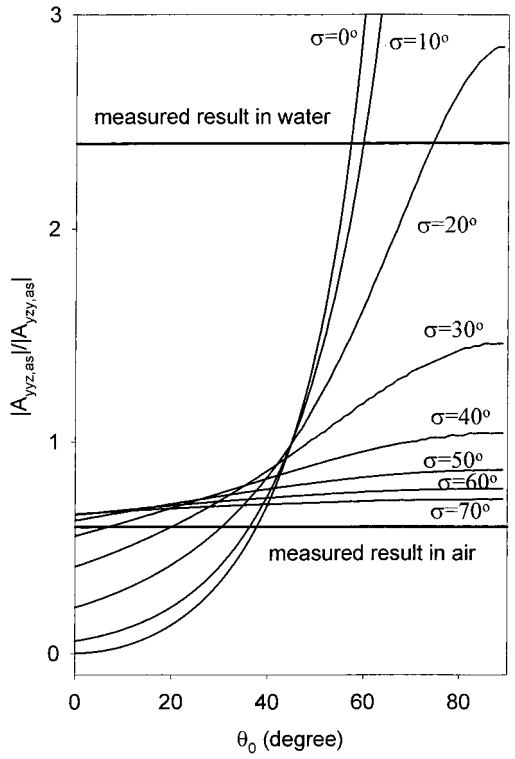

Figure 2. Calculated $|A_{yyz,as}|/|A_{yzy,as}|$ of methyl group as a function of orientation angle θ_0 and angle distribution σ.

calculations later) are quite similar to those listed in Table 1. Here we consider that the visible input beam has a δ function line shape, the input IR beam has a Lorentzian line shape with a width of 6 cm^{-1} in the wavenumber range (2800−3100 cm^{-1}) of the spectra shown in Figure 1. We fitted SFG spectra by convoluting these line shapes along with eqs 3.2 and 3.3. The fitting also includes the O−H stretches of water molecules to describe the baseline of the PBMA spectra in water above 3000 cm^{-1} (not shown in Table 1). In Table 1, the measured second-order nonlinear susceptibility tensor components have been already calibrated against the reference and are expressed as absolute values in SI units.[39,40]

To explore the possible range of orientation angles and orientation angle distribution within the assumption of a Gaussian distribution, we calculated the behavior of the ratio $|A_{yyz,as}|/|A_{yzy,as}|$ as a function of θ_0 for certain values of σ of the distribution using eq 3.5. The resulting curves are shown in Figure 2, along with the experimentally determined ratios (0.6 in air and 2.4 in water). With the help of Figure 2, we can determine the extremal distributions (i.e., the narrowest and the widest).

In water the measured $|A_{yyz,as}|/|A_{yzy,as}|$ value is far from the ratio characteristic for the magic angle;[28] therefore, experimental error should not affect the results too much (see detailed discussion below). If we assume that the angle distribution is a δ function, then Figure 2 gives $\theta_0 = 57°$. If we assume that $\theta_0 = 90°$, the angle distribution σ has the largest possible value of 23°. Actually the latter is not a practical orientation angle, since the SFG intensity should be zero. Therefore, the real orientation angle distribution should be between the two extremes of $\theta_0 = 57°$ with a δ distribution and $\theta_0 = 90°$ with $\sigma = 23°$.

Now let us look at methyl groups on the PBMA surface in air. From Figure 2 we see that the extremal orientation distributions are a δ distribution with $\theta_0 = 37°$ and a distribution with $\theta_0 = 0°$ and $\sigma = 45°$. Unfortunately, the measured value of $|A_{yyz,as}|/|A_{yzy,as}|$ in air is not very different from the magic angle value. From Figure 2 it follows that small experimental error may substantially affect the deduced results. In addition, the value of $|A_{yyz,as}|$ is small and can be easily affected by the measurement or spectral fitting error. Therefore, we have also calculated the ratio of $|\chi^{(2)}_{yyz,s}|/|\chi^{(2)}_{yzy,as}|$ and used an analysis similar to that of $|A_{yyz,as}|/|A_{yzy,as}|$. We managed to confirm the above results, and thus we believe that the information deduced about orientation angle and angle distribution is reliable.

Again, we emphasize that from the intensity ratio of ssp and sps spectra, the parameters of the distribution function cannot be determined uniquely. One value of $|A_{yyz,as}|/|A_{yzy,as}|$ can correspond to different combinations of θ_0 and σ. However, ranges of possible orientation angle and orientation angle distribution have been deduced from $|A_{yyz,as}|/|A_{yzy,as}|$. Theoretically, if the absolute intensity of the SFG spectra can be accurately measured, from its combination with the measured spectral intensity ratio in the ssp and sps SFG spectra, both parameters of the orientation angle distribution θ_0 and σ can be deduced. We describe now how to include the absolute spectral intensity in the calculation.

We calculated $|A_{yyz,s}|^2$ for the methyl group with the help of eqs 3.2, 3.3, and 3.4 as a function of θ_0 using the corresponding σ values deduced from Figure 2. In this way we took into account the information already available from the ratio measurement during evaluation of the absolute intensity measurement. For the calculation, we used the molecular hyperpolarizability components listed in refs 39 and 40. The curves calculated by using different values of surface density of methyl groups, as well as the measured intensities, are shown in Figures 3 and 4 for the PBMA/air and PBMA/water interfaces, respectively. As we stated, no apparent backbone change occurs when PBMA surface contacts water. We believe that the assumption of equal coverage of side chain methyl groups on the PBMA surface in air and in water is valid. Figure 3 shows that the possible values of N_s are between 5.4×10^{14} to 7.3×10^{14} cm^{-2}. Figure 4 indicates that N_s should be larger than 6.8×10^{14} cm^{-2}. Assuming the same surface density of methyl groups on PBMA surfaces in air and in water, we can deduce the possible range of this density from Figures 3 and 4. It is deduced to be a small range from 6.8×10^{14} to 7.3×10^{14} cm^{-2}. We will use an intermediate value 7.0×10^{14} cm^{-2} in the following calculation. To accurately calculate the absolute intensity of the methyl symmetric stretching peak, we have to consider the interference of Fermi resonance, which may "borrow" intensity from the symmetric stretch.[25] Here, we believe that the Fermi resonance effect would be similar for the ssp spectra of PBMA in air and in water, and it has already been accounted for in the choice of the surface density of methyl groups. Our choice of surface density also includes the local field correction.[27,39] From the measured spectral intensity value and the calculated intensity curves using $N_s = 7.0 \times 10^{14}$ cm^{-2} (black dots in Figures 3 and 4), the orientation angle distribution can be obtained. The distribution functions deduced in this way

(40) Oh-e, M.; Lvovsky, A. I.; Wei, X.; Shen, Y. R. *J. Chem. Phys.* **2000**, *113*, 8827.

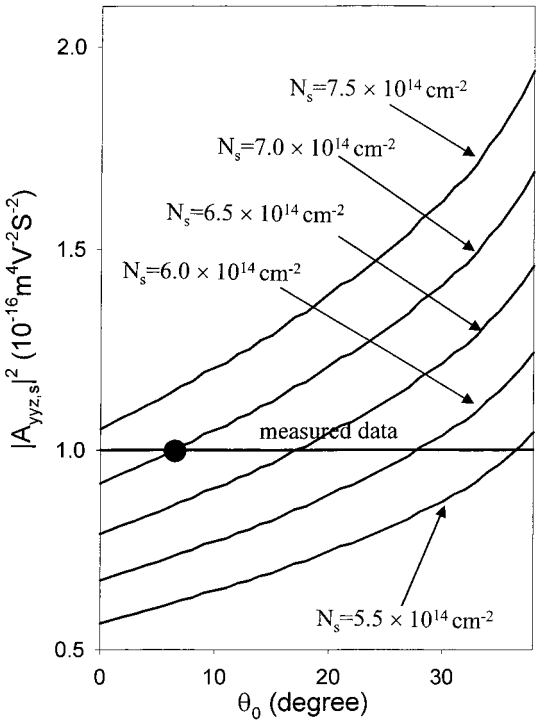

Figure 3. Calculated values of $|A_{yyz,s}|^2$ as a function of possible orientation angles θ_0 and corresponding angle distribution σ, deduced from Figure 2, of methyl groups at the PBMA/air interface using different surface density values.

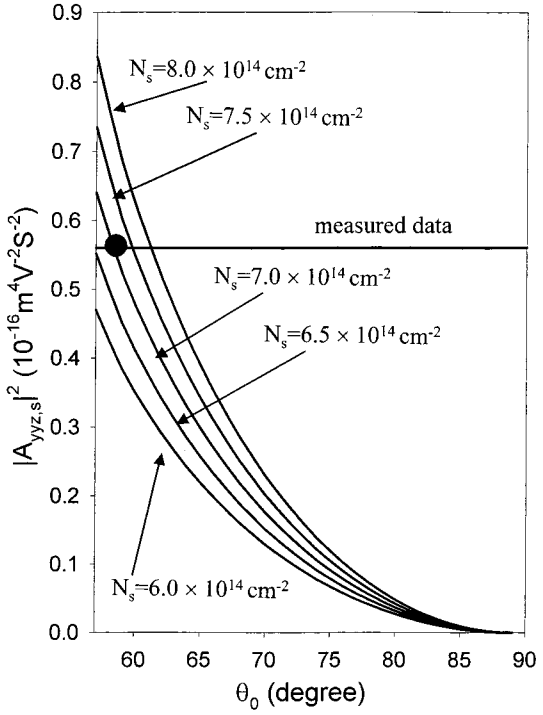

Figure 4. Calculated values of $|A_{yyz,s}|^2$ as a function of possible orientation angles θ_0 and corresponding angle distribution σ, deduced from Figure 2, of methyl groups at the PBMA/water interface using different surface density values.

for side chain methyl groups on the PBMA surface in air and in water are shown in Figure 5 using the normalized distribution population of $N_s(\theta) = N_s f(\theta) \sin(\theta)$.

From Figure 5, it is quite clear that the side chain methyl groups tend to stand up on the surface in air with a quite wide

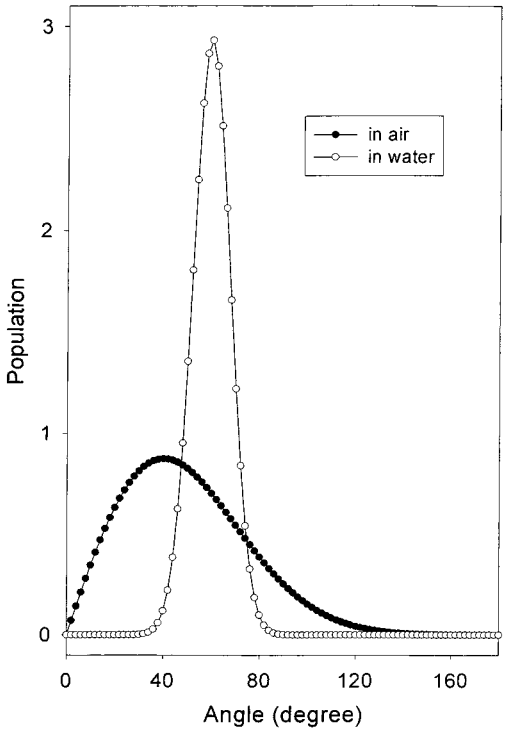

Figure 5. Angle distributions of side chain methyl groups on the PBMA surface in air and in water calculated with the assumption of a Gaussian distribution.

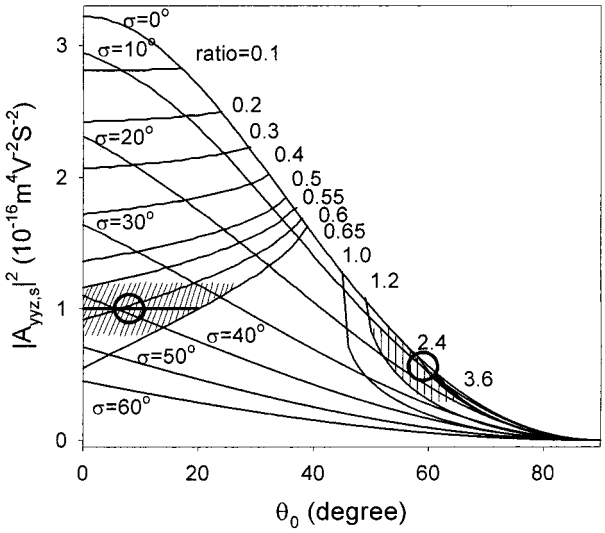

Figure 6. Analysis of the effect of experimental error on determination of the parameters of the Gaussian distribution function.

angular distribution. On the other hand, they tend to tilt more toward the surface in water, with a much narrower distribution, indicating that the surface in water is more ordered.

Since experimental error may affect the deduced results, further analysis is necessary. Figure 6 displays both the value of $|A_{yyz,s}|^2$ and the ratio of $|A_{yyz,as}|/|A_{yzy,as}|$ as functions of the orientation angle θ_0 and distribution width σ. The measured results, the centers of two circles, are also shown in Figure 6 for the side chain methyl groups on the PBMA surface in air and in water. From these measured results, we have deduced the distributions above, which are shown in Figure 5. Figure 6 illustrates clearly how the experimental error affects our deduced

results about the orientation distribution. The hatched area on the left shows the possible distribution (θ_0 and σ) of methyl groups in air for measured $|A_{yyz,s}|^2$ between 0.8 and 1.2 (10^{-16} m^4 V^{-2} s^{-2}), and measured $|A^{(2)}_{yyz,as}|/|A^{(2)}_{yzy,as}|$ between 0.55 and 0.65. In air, these measured experimental errors can induce some uncertainties for the results. In water, similar experimental error will have less effect on our deduced results. For measured $|A_{yyz,s}|^2$ between 0.49 and 0.69 (10^{-16} m^4 V^{-2} s^{-2}), and measured $|A_{yyz,as}|/|A_{yzy,as}|$ between 2.2 and 2.6, the possible range of distribution is very narrow, inside the right black circle. It is too narrow to be clearly shown in Figure 6. From Figure 6, we can see that even with these experimental errors, the conclusion that the methyl groups in water orientate more toward the surface and have a narrower orientation distribution would not change. Because the spectral intensities of the SFG spectra of the polymer/water interface are weaker, there may be more uncertainties introduced by spectral fitting. Therefore, we increased the error bars to accommodate ±50% error in both intensity ratio and absolute intensity measurements of the PBMA/water interface. The possible distribution (θ_0 and σ) induced by such errors is illustrated by the hatched area on the right in Figure 6. Figure 6 shows clearly that even including such large error bars, our conclusions about orientation and orientation distribution are still valid.

As we mentioned in the Introduction, we obtained some information on how reasonable the choice of the Gaussian distribution function can be. The maximum entropy approach accommodates a broader range of possible functions. Therefore, we compare the resulting maximum entropy distribution with the Gaussian function just determined. In addition, the analysis of the effect of possible experimental error is repeated.

After measuring the absolute intensity of the symmetric stretch band and the value of $|A_{yyz,as}|/|A_{yzy,as}|$, as we have done above, we can determine the orientation angle distribution function of the side chain methyl group. Now the characteristics of the problem allow for direct numerical solution, instead of the graphical deduction of the distribution described above. Therefore, we regard the distribution again as a function of cos θ and rewrite eq 3.4 so that the measured value $\chi^{(2)}_{yyz,s}$ is related to the first and the third moments of the distribution $f(\cos\theta)$ (see eq 3.8) by:

$$\chi^{(2)}_{yyz,s} = \frac{1}{2} N_s \alpha_{ccc}[(1+r)\langle\cos\theta\rangle - (1-r)\langle\cos^3\theta\rangle] = \frac{1}{2} N_s \alpha_{ccc} \langle\cos\theta\rangle[1 + r - \gamma(1-r)] \quad (4.1)$$

The parameter γ is defined as $\gamma = \langle\cos^3\theta\rangle/\langle\cos\theta\rangle$, which can be obtained from the measured ratio of $|\chi^{(2)}_{yyz,as}|/|\chi^{(2)}_{yzy,as}|$ since

$$\frac{|\chi^{(2)}_{yyz,as}|}{|\chi^{(2)}_{yzy,as}|} = \frac{|\langle\cos\theta\rangle - \langle\cos^3\theta\rangle|}{|\langle\cos^3\theta\rangle|} = \left|\frac{\langle\cos\theta\rangle - \langle\cos^3\theta\rangle}{\langle\cos^3\theta\rangle}\right| = \left|\frac{1}{\gamma} - 1\right| \quad (4.2)$$

As we can see from eq 4.1, by measuring the absolute value of $|A_{yyz,s}|^2$, and inserting γ deduced from eq 4.2, we can calculate $\langle\cos\theta\rangle$ and $\langle\cos^3\theta\rangle$. The unknown coefficients a_0, a_1, and a_2 of the distribution function eq 3.11 can then be found as the numerical solution of the following set of equations:

$$1 = \int_{-1}^{1} \exp(a_0 + a_1 x + a_2 x^2) dx \quad (4.3)$$

$$\langle\cos\theta\rangle = \int_{-1}^{1} x \exp(a_0 + a_1 x + a_2 x^2) dx \quad (4.4)$$

$$\langle\cos^3\theta\rangle = \int_{-1}^{1} x^3 \exp(a_0 + a_1 x + a_2 x^2) dx \quad (4.5)$$

where the substitution of $x = \cos\theta$ was applied for convenience. To find the numerical solution of the above set, the integrals were evaluated using a 16-point Gauss−Legendre formula. The calculated angle distribution function $f(\theta)\sin\theta$ for the side chain methyl groups on the PBMA surface in air is shown in Figure 7, along with the corresponding Gaussian distribution deduced above. The Gaussian distribution is very close to the maximum entropy distribution, indicating that the Gaussian function is a good approximation for the distribution function.

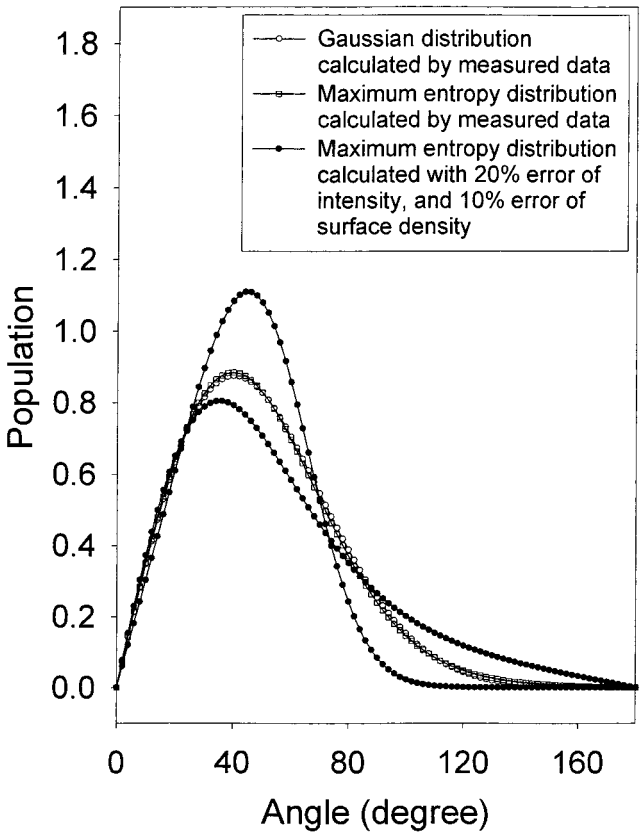

Figure 7. Comparison between orientation angle distributions of side chain methyl groups on the PBMA surface in air deduced using the Gaussian distribution and the maximum entropy distribution, showing the extremal maximum entropy distributions allowed by the experimental error ranges.

The effect of experimental error was evaluated by estimating the error of the $|A_{ijk}|^2$ values deduced from the measured spectra to be ±20%, and the error of N_s to be ±10%. In Figure 7, the narrowest and widest possible distributions compatible with these error ranges are also plotted. It can be seen that even with such big error bars, the angle distribution does not vary substantially. Figure 8 shows the orientation angle distribution of side chain methyl groups on the PBMA surface in water. Similar to the air case, the angle distributions calculated by the maximum entropy distribution and the Gaussian distribution are

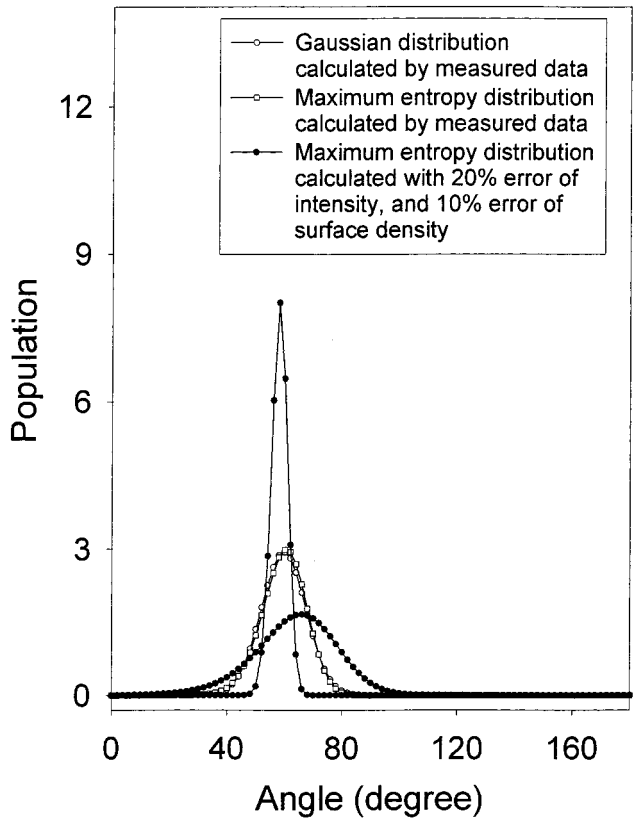

Figure 8. Comparison between orientation angle distributions of side chain methyl groups on the PBMA surface in water deduced using the Gaussian distribution and the maximum entropy distribution, showing the extremal maximum entropy distributions allowed by the experimental error ranges.

quite similar. The effect of experimental error on the measured angle distribution has been analyzed following the PBMA surface in air, and the resulting distributions are also plotted in Figure 8. The narrowest distribution in the figure is just a schematic representation of a δ-distribution, which is the narrowest distribution consistent with the above given experimental error range.

Finally, we emphasize that the maximum entropy distribution in the present three-parameter form (eq 3.11) as well as the Gaussian distribution are only approximations to the real distribution function. As the results deduced from these two functions are quite similar, we believe both of them are reasonable estimations of the real distribution. According to eq 3.10, however, including the cubic term in $\cos\theta$ may improve the approximation. It can be done by directly measuring $\langle\cos^2\theta\rangle$, when possible, in addition to $\langle\cos\theta\rangle$ and $\langle\cos^3\theta\rangle$ deduced from SFG measurements.

5. Conclusions

Molecular surface structures of PBMA in air and in water have been studied by SFG. In water, the PBMA surface becomes more ordered, evidenced by a narrower angular distribution of the surface side chain methyl groups. These side chain methyl groups tilt more toward the surface in water, while in air they tend to stand up. The orientation angle distribution of side chain methyl groups is deduced from the intensity ratio of ssp and sps SFG spectra and from the absolute ssp SFG spectral intensity. Two distribution functions, a Gaussian distribution and a maximum entropy distribution, have been applied to calculate the angle distribution. Calculated results from the two functions are similar, indicating that the Gaussian distribution is a good approximation for the orientation angle distribution.

Acknowledgment. This work is supported by start-up funds from the University of Michigan. We acknowledge the financial support for Dr. Paszti from the Chemical Research Center of the Hungarian Academy of Sciences and the Optical Physics Interdisciplinary Laboratory of the University of Michigan. We thank Dr. Lee Richter for his inspiring suggestions.

JA012387R